Predicting the Shear Strength of Fiber Reinforced Concrete Corbels Via Support Vector Machines

Ahmet Emin KURTOGLU

Istanbul Gelisim University, Civil Engineering Department, Avcilar, Istanbul, TURKEY

Abstract: Precast corbels are commonly preferred structural members in industrial buildings. In this study, a novel application of support vector machines (SVM) is employed for the prediction of ultimate shear strength of fiber reinforced corbels, for the first time in literature. SVM models are developed and analyzed using a database of available test results in literature. Predictions of the selected model are compared against the test results and those of available model proposed by Fattuhi (1994). Proposed model has the capability to predict the shear strength of both steel fiber reinforced concrete (SFRC) and glass fiber reinforced concrete (GFRC) corbels. Additionally, a parametric study with a wide range of variables is carried out to test the effect of each parameter on the shear strength. The results confirm the high prediction capacity of proposed model.

Keywords: Support vector machines, reinforced concrete corbel, fiber reinforced concrete, steel fiber, glass fiber, shear strength.

Lifli Betonarme Kısa Konsolların Kesme Dayanımının Destek Vektör Makineleri ile Tahmini

Özet: Prefabrik kısa konsollar, özellikle sanayi yapılarında sıkça tercih edilen yapı elemanlarıdır. Bu çalışmada, lifli betonarme kısa konsolların kesme dayanımı, literatürde ilk defa, destek vektör makineleri (DVM) ile tahmin edilmiştir. Mevcut deneysel veriler kullanılarak DVM modelleri oluşturulmuş ve tahmin performansları analiz edilmiştir. Seçilen modelin tahminleri, deney sonuçları ve literatürde mevcut olan modelin (Fattuhi, 1994) tahminleri ile karşılaştırılmıştır. Model, çelik lifli kısa konsolların yanı sıra cam lifli konsolların taşıma kapasitelerini de tahmin edebilmektedir. Ayrıca model, her bir girdi parametresinin etkisini incelemek amacıyla, parametrik analize tabi tutulmuştur. Sonuçlar, önerilen modelin yüksek tahmin kapasitesine sahip olduğunu göstermektedir.

Anahtar Kelimeler: Destek vektör makineleri, betonarme kısa konsol, lifli betonarme, çelik lif, cam lif, kesme dayanımı.

1. INTRODUCTION

Precast concrete elements are commonly preferred by designers in building and bridge construction. Precast corbels, an example of such elements, transfer the loads from slabs and beams to columns or walls. In general, a corbel is either project out from a column or structural wall or is designed as the overhanging portion of a beam. (Fig. 1). Corbels can be provided to support rails which transfer heavy loads from moving cranes in heavy–duty factory workshops. Corbels are also provided at the cantilevered end of the girders in double cantilever balanced reinforced concrete bridges to support the end spans of the bridge. The span-to-depth ratio of a corbel is usually equal to one or smaller than one ($a/d \leq 1$).

In order to improve the properties of concrete, various type of fibers are added to form fiber reinforced concrete (FRC). Although the structural behavior of FRC elements depends on the mechanical properties of the composite, fibers can be considered as reinforcement spread out all over the depth of a member. The addition of steel fibers to the concrete allows for a substantial increase of the shear strength. The effectiveness of fiber reinforcement to increase shear resistance, is dependent on several factors, including matrix properties, fiber properties (material properties, aspect ratio, and shape), fiber content, and bond stress versus slip response of fibers. Fiber contents are generally within the range of 0.5% - 2% by the weight of fiber. Main disadvantage of using fibers in concrete is that it reduces the workability of concrete. However, additives are used to overcome this problem.

Hydraulic cement with aggregate (fine or course) and discrete steel fibers, as shown in Fig. 2a, are used to produce steel fiber reinforced concrete (SFRC). Steel fibers for SFRC are manufactured as short, discrete lengths of steel with an aspect ratio (length-to-diameter ratio) varying between 20 and 100. Steel fibers are small enough to be dispersed in fresh concrete mix, randomly [1].

Figure 1. Corbels in an industrial building.

The addition of steel fiber in concrete leads to a number of enhancements in the behaviour of structural member. In compression, steel fibers do not significantly affect the ascending curve of the compressive stress-strain response. However, they cause the descending post-peak response curve to decline in a shallower fashion than the curve of plain concrete, resulting in an increased ductility and toughness [2]. The researchers observed an enhancement of only 15% in compression. However, the peak strain increases significantly with the provision of steel fibers [1-3].

On the other hand, the addition of steel fibers induces a much more noticeable effect on the tensile behavior. The strain softening behavior is observed in the concrete with typical fiber volume content. This results in the composite having greater ductility and energy absorption capabilities than the plain concrete. In addition, because the fibers bridge the cracks in the composite and aid in the transfer of forces across the cracks, crack widths are less than those in plain concrete. If the reinforcing bars are present, multiple cracks can form even for a strain-softening material. As compared to the plain concrete, there will be more cracks at shorter spacing and with smaller widths [4].

Various universal products are manufactured using alkali resistant glass fibers. The provision of glass fibers in concrete lead to various behavioral advantages such as high flexural strength, ability to reproduce, low maintenance requirements, and environmental friendliness. As depicted in Fig. 2b, glass fibers are unorganized and are easily dispersed in fresh concrete thanks to their thin and soft nature. The diameter of thin glass fiber or filament ranges from approximately 3 to 24 µm. The 17 µm fiber diameter is most commonly used for FRC products for structural engineering [1].

Figure 2. (a) Steel fibers (b) Glass fibers.

2. FIBER REINFORCED CONCRETE (FRC) CORBELS

In FRC, fibers can be considered as tiny reinforcements spread out in the concrete member. The effect of fiber addition is dependent upon several factors such as matrix properties, fiber properties (material properties, aspect ratio, and shape), fiber content, and bond stress versus slip response of fibers.

2.1 Steel Fiber Reinforced Concrete (SFRC) Corbels

Fattuhi ve Hughes [5-9] conducted a series of experiments on the load carrying capacities of SFRC corbels produced with normal strength concrete. They investigated several factors (tensile and compressive strength of concrete, steel fiber volume fraction, shear span, fiber aspect ratio, effective depth, reinforcement ratio) and observed the mechanical response of SFRC corbels. Fattuhi (1994) also studied the mechanical behavior of normal strength SFRC corbels with trapezoidal shape [7].

Flexural behavior of fibrous reinforced concrete corbels are investigated experimentally by Campione et al. (2007). The authors also proposed simple analytical expressions for bearing capacity by considering the shear contribution due to steel reinforcements and fibers [10]. Also, the combined effect of horizontal and vertical loading is investigated [11].

Fattuhi (1994) proposed a practical empirical formulation based on experimental results, which predicts the ultimate load capacity of SFRC corbels by considering some parameters which influence the mechanical behavior [7]. The expression of the formula is:

$$V_{k,Dnk1} = k_1 bh (f_{ct})^{k_2} (\frac{a}{h})^{k_3} (\frac{f_y}{f_{cu}})^{k_4} (\frac{d}{h})^{k_5} (\rho)^{k_6} \qquad (1)$$

where $k_1 = 57.292$, $k_2 = 0.315$ $k_3 = -0.812$, $k_4 = -0.049$, $k_5 = 0.678$, $k_6 = 0.626$, b is the total width of rectangular section in mm, h is the overall depth of corbel in mm, d is effective depth of main bars in mm, f_{ct} is average splitting tensile strength in MPa, f_y is the yield strength of main bars in MPa, f_{cu} is average cube compressive strength of concrete in MPa.

Fattuhi (1994) also proposed two more models namely as "Flexural Model" and "Truss Model" for the load carrying capacities of steel fiber reinforced concrete corbels [7]. Basic formulas for these models are:

Flexural Model

$$V_{MODEL} = \frac{f_y A_s}{a}(d - \frac{a_1}{2}) + \frac{k_0 f_{ct} b}{2a}(h - \frac{a_1}{\beta_1})(h + \frac{a_1}{\beta_1} - a_1) \tag{2}$$

where

$$k_0 = \frac{9.519}{(f_c)^{0.957}} \quad ve \quad a_1 = \frac{f_y A_s + k_0 f_{ct} hb}{0.85 f_c b + k_0 f_{ct}(\frac{b}{\beta_1})} \tag{3}$$

Truss Model

$$V_{MODEL} = \frac{f_y A_s (d - (\frac{l \sin \beta}{2})) + 0.5 k_0 f_{ct} bh(h - (l \sin \beta))}{a + 0.5(l \sin \beta) \cot \beta} \tag{4}$$

where

$$l \sin \beta = \frac{f_y A_s + k_0 f_{ct} bh}{0.85 f_c b + k_0 f_{ct} b} \tag{5}$$

and $\cot \beta$ is determined with following equation:

$$0.425 f_c b (l \sin \beta)^2 \cot^2 \beta + 0.85 f_c ab(l \sin \beta) \cot \beta - f_y A_s (d - \frac{(l \sin \beta)}{2})$$
$$- 0.5 k_0 f_{ct} bh(h - (l \sin \beta)) = 0 \tag{6}$$

In the equations, b and h are width and height of the corbel in mm, respectively, f_{ct} is the splitting tensile strength of fibrous concrete in MPa, d/a is the reciprocal of the shear span-to-depth ratio and A_s is sectional area of main reinforcement. Other parameters are explained in Fig. 3a. Ultimate load carrying capacity of SFRC corbel is in Newtons.

High strength concrete SFRC corbels were also studied by various researchers. Muhammed (1998) investigated the performance of SFRC high strength corbels with trapezoidal form under monotonic and cyclic loading [12]. Yang et al. (2011) studied the effect of steel fibers on the serviceability of reinforced concrete corbels [13].
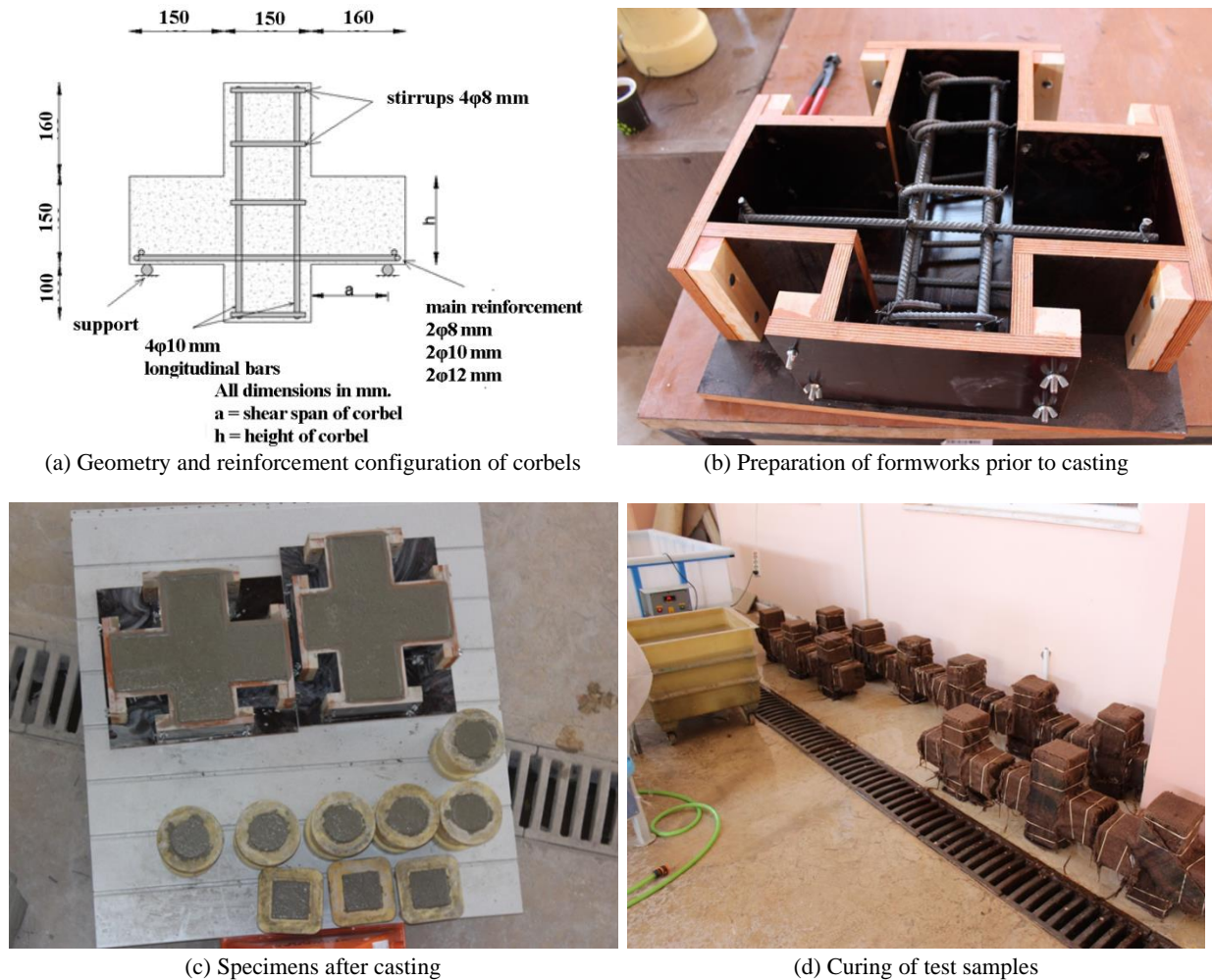
(a) Geometry and reinforcement configuration of corbels

(b) Preparation of formworks prior to casting

(c) Specimens after casting

(d) Curing of test samples

Figure 3. Preparation of corbel specimens [14].

Kurtoglu et al. (2017) carried out an investigation on shear strength of SFRC corbels whose test configuration is shown in Fig. 3a [14]. A total of twenty-four specimens were prepared for experiments, sixteen of which were prepared with SFRC while the remaining six specimens contained plain concrete. Six 10mm x 20mm cylinder sample and three 10mm x 10mm cube samples were prepared for two corbels (Fig. 3c). Three of the cylinders were used to measure the splitting tensile strength of the concrete; other three cylinders were used to measure the compressive strength of the concrete. Three cube samples were prepared to measure the cubic compressive strength of the concrete. Six cylinder and three cube samples and two corbel specimens were produced as a result of one concreting batch. The formworks were removed

one day after the concreting process and the corbels were covered with a special textile for curing process. Corbels and corresponding samples were watered during 28 days to reach the target strength (Fig. 3d). The corbels and samples were tested in a loading frame after 28 days. Corbels were tested using a 500 kN capacity loading frame. Corresponding samples were also tested to measure the compressive strength and tensile strength. Compressive strength and tensile strengths were tested in a 2000 kN capacity concrete press machine.

Fig. 4a depicts an example test specimen and Fig. 4b shows the crack pattern on a random specimen after the experiment. As concluded by the authors, provision of steel fibers yields an increase in ductility and ultimate strength of

corbels. It is also highlighted that steel fibers can be an alternative to stirrups as a secondary reinforcement. To increase the ductility, however, provision of steel fibers cannot be

solely adequate and, the other factors such as proper selection of concrete class, reinforcement diameter, span and fiber ratio are also significantly effective [14].
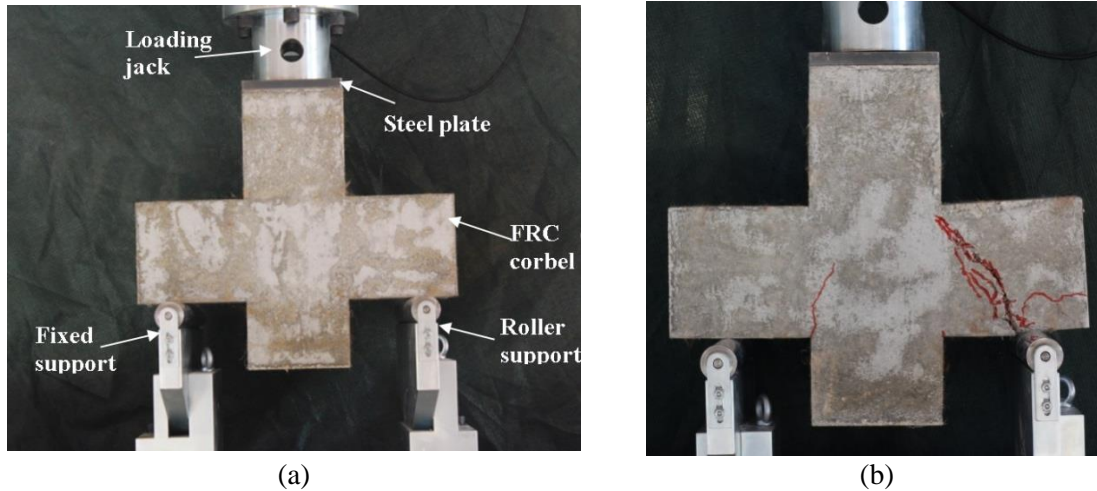

Figure 4. (a) Test setup (b) Crack pattern [14].

2.2 Glass Fiber Reinforced Concrete (GFRC) Corbels

So far, literature does not provide any prominent information regarding the strength of GFRC corbels as opposed to the research on corbels with SFRC. The only research was provided by Kurtoglu et al. (2017), in which nine normal strength and nine high strength GFRC corbel samples were investigated experimentally [14].

For testing, a universal testing machine with 500 kN capacity was utilized and the samples were loaded concentrically. Fig. 4a and Fig. 4b show the test setup prior to testing and crack pattern, respectively. Table A.1. lists the material and geometry properties as well as the test results (ultimate shear strength, V_{ke}). Consequently, provision of glass fibers in corbels yielded an increase in post cracking load and ultimate load capacity. Additionally, brittle failure was observed in plain corbels while GFRC corbels failed in ductile manner [14].

3. OVERVIEW ON SUPPORT VECTOR MACHINES (SVM)

Support vector machines (SVM) is an artificial intelligence based method, which was initially developed by Boser et al. (1992) for classification problems [15]. Researchers also employed this technique for solving the regression problems and called it support vector regression (SVR).

Besides its solid numerical basis in statistical learning theory, support vector machines have showed extremely competing performance in several applications, e.g., face recognition, text mining, bioinformatics and image processing. This fact has proven that SVMs are one of the state-of-the-art approaches for data mining and machine learning, together with some other soft computing methods, e.g., fuzzy systems and neural networks[16].

The principal of SVM is based on obtaining the most suitable linear function that will separate two classes of data. This function ignores the errors in a predetermined range and tries to obtain the optimum hyper plane between two

classes of data. The main goal of SVR is to find a function which can estimate the real output values with maximum of (ε) error and to obtain two hyper planes parallel to this function. The distance between these planes should be minimum [17].

3.1 Support Vector Regression (SVR)

Initially, SVM were introduced for solving the classification problems. Researchers started utilizing SVM for regression problems by preserving the entire algorithm used and called this support vector regression (SVR). A function

named ε-insensitive loss function that neglects errors that are inside a definite distance of the exact value is able to supervise a parametric quantity that is equal to the margin parameter for separating hyper planes. For a given set of training data in SVR, the main purpose is to obtain a function with maximum difference from the exact found targets for all the training data, and at the same time, is at most flat i.e., we do not focus on errors as long as they are less than a certain amount, but any deviation larger than a this amount is not acceptable (Chen et al., 2004). The (linear) -insensitive loss function $L(x, y, f)$ is described as

$$L^{\varepsilon}(x,y,f) = |y - f(x)|_{\varepsilon} = \begin{cases} 0 & if |y - f(x)| \leq \varepsilon \\ |y - f(x)| - \varepsilon & otherwise \end{cases} \tag{7a}$$

where f is a real-valued function on a x and the quadratic ε-insensitive loss is defined by

$$L_2^{\varepsilon}(x,y,f) = |y - f(x)|_{\varepsilon}^2 \tag{7b}$$

Figure 5 illustrates the form of linear and quadratic ε-insensitive loss function for zero and non-zero ε.
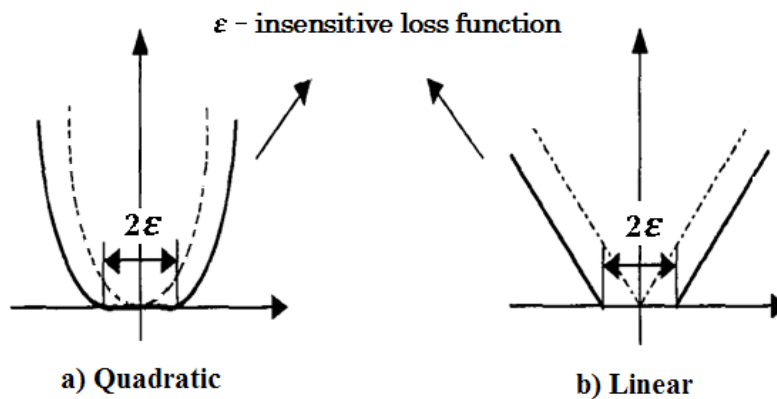
Figure 5. The form of linear and quadratic ε-insensitive loss function for zero and non-zero ε.

The loss function $L(y, f(x, \omega))$ determines the performance of accuracy. Performing linear regression in the high-dimension feature space by the use of ε-insensitive loss function, SVM attempts to decrease model complexity by performing the minimization of $\|\omega\|^2$. By introducing (non-negative) slack variables $\xi_j, \xi_i^* i = 1,...n$

$$L(y, f(x, \omega)) = |y - f(x)|_{\varepsilon}^2$$

$$L_2^{\varepsilon}(x, y, f) = |y - f(x)|_{\varepsilon}^2 \tag{7c}$$

to determine the deviation of training data outside ε-zone. Following formulation is utilized for the minimization of SVM regression:

$$\frac{1}{2}\|\omega\|^2 + c\sum_{i=1}^{n}(\xi_{i+}\xi_i^*) \text{ subject to } \xi_j, \xi_i^* i = 1,...n \tag{7d}$$

$$\xi_j, \xi_i^* i = 1,...n \tag{7e}$$

The solution of this optimization problem can be found by transforming it into the dual problem:

$$f(x) = \sum_{i=1}^{n_{sv}}(\alpha_j - \alpha_i^*)K(x_j, x) + b \text{ subject to } 0 \le \alpha_i^* \le C, 0 \le \alpha_j \le C \tag{7f}$$

where n_{sv} is the number of support vectors (SVs), a_i^* and a_j are the Lagrange multipliers and $K(x_j, x)$ is a kernel function and b is the bias term. Generalization capability (accuracy of estimation) of SVM is dependent on a proper setting of meta-parameters C, ε and the kernel parameters. Current software applications usually allow users to define meta-parameters of SVM regression [18].

Parameter C controls the exchange between the model complexity as well as the degree to which deviations larger than ε are tolerated in optimization formulation. Parameter ε describes Linear kernel function:

the width of ε-insensitive zone, which is utilized to fit the training data. The number of SVs used to create the regression function can be affected by the value of ε. The fewer SVs are obtained by choosing the bigger ε. On the other hand, greater ε-insensitive values cause more 'flat' predictions. Although in different ways, both C and ε values affect model complexity (flatness) [18].

Although various kernel functions are available in machine learning theory, four kernel functions are employed in this study:

$$K(x_i, x) = x_i x \tag{8a}$$

Polinomial kernel function:

$$K(x_i, x) = (x_i(x+1))^d \tag{8b}$$

Radial based kernel function:

$$K(x_i, x) = \exp\left[-\frac{(x_i - x)(x_i - x)}{2\sigma^2}\right] \tag{8c}$$

Sigmoid kernel function:

$$K(x_i, x) = \tanh(x_i(x+1)) \tag{8d}$$

where x_i and x are training and testing input, respectively, σ is the Gaussian kernel function width and d is the polynomial degree of kernel function.

Previously, SVM was employed in several civil engineering applications e.g., prediction of fresh concrete properties, mechanical characteristics of concrete, damage detection, corrosion, self-compacting concrete (SCC) properties and rainfall-runoff modeling. Zhang and Song (2012) employed SVM to predict the residual mechanical characteristics of fly ash concrete specimens exposed acidic environment [19]. Yang et al. (2014) investigated the mechanical properties of corroded concrete and performed tests on specimens under repeated loads. Deflection and maximum crack with parameters were predicted using least squares support vector machines (LS-SVM) [20]. Cao et al. (2013) presented a predictive SVM based model for elastic modulus of SCC [21]. Also, a SVM based approach was implemented for structural reliability analysis by Li and Lu (2007) [22]. On the other hand, Okkan and Serbes (2012) successfully implemented LS-SVM approach to predict the runoff values and compared the results to those of artificial neural networks (ANN) based models [23]. Çevik et al. (2015) presented a review that investigates the studies on the use of SVM in structural engineering [24]. The literature incorporates model proposals based on regression [7] and artificial neural networks [25]. However, a unified model that predicts shear strength of both SFRC and GFRC corbels is not present until recently. This research is the pioneer study that incorporates the SVM-based estimation of shear strength of both SFRC and GFRC corbels.

4. NUMERICAL APPLICATION

In this paper, emphasis was placed on obtaining a unified SVM model to estimate the shear strength of FRC corbels. A total of 126 data set was used for model creation, whose input variables were fiber type (1-steel fiber, 2-glass fiber), span-to-depth ratio (a/d), reinforcement ratio (ρ), reinforcement tensile strength (f_y), concrete compressive strength (f_{cu}), concrete tensile strength (f_t) and fiber volume ratio (v_f). The output parameter was shear strength (V_k). Input parameters contained concrete compressive strength of cylinder test specimens for both normal strength and high strength concrete. The ranges of input parameters are listed in Table 1. Furthermore, Fig. 6 illustrates the data distribution of input parameters and no abnormal fluctuation was observed.

Table 1. Statistical values of test data.

	a/d	ρ (%)	f_y (MPa)	f_{cu} (MPa)	f_t (MPa)	v_f (%)	V_k (kN)
Max.	1.47	1.53	560.00	92.79	9.28	2.50	179.00
Min.	0.43	0.44	448.70	22.30	1.90	0.00	37.57
Average	0.88	0.84	491.47	38.08	4.74	1.21	103.06
St. Dev.	0.20	0.32	45.84	16.47	1.17	0.74	32.46
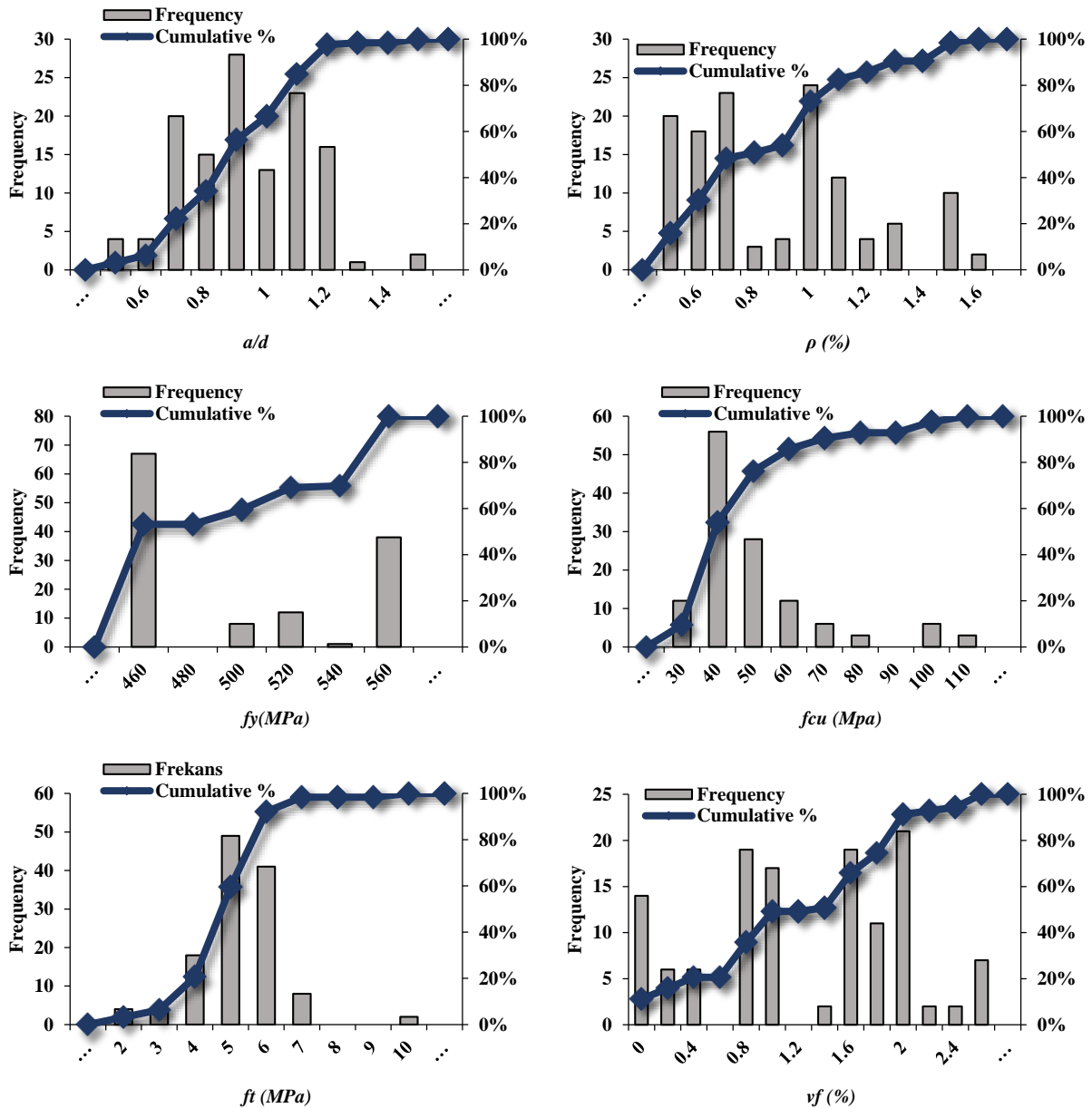
Figure 6. Distribution charts for input variables.

SVM models were created using a commercially available software named DTREG [26]. Selection optimal model parameters is of great importance in SVM. Hence, two different approaches (grid search and pattern search) were implemented to find the optimum model parameters. During the grid search, the program evaluates the search area predefined by the user. Pattern search, on the other hand, is based on searching values, starting from the center and trying the steps in both directions for each

parameter. This process continues until the predefined search criteria is achieved. Since the model is evaluated at a too many number of grid points, grid searches require a large computation time and performance. Pattern search requires less computation time as compared to grid search.

Model creation process has been conducted by using two different kernel types (Epsilon-SVR and Nu-SVR) and four different SVM kernel

functions (Linear, Polynomial, Radial basis and Sigmoid function). To overcome the problem of overfitting, v-fold cross validation was applied and the data was separated as testing and training based on random selection. 25% of data was selected as testing set based on random selection, operated by the software automatically. Table 2 lists the input parameters and results for each SVM model.

Table 2. Input and statistical values for developed SVR models.

SVR model No.	SVR model type	SVR kernel function	Number of support vectors	Parameter values				RMSE		CoV		R²	
				C	P	Coeff0	Gamma	Training	Testing	Training	Testing	Training	Testing
1	Epsilon-SVR	Linear	126	150.48	0.002	-	-	10.5	10.97	0.101	0.106	0.894	0.884
2	Epsilon-SVR	Polinomial degree = 3	101	0.1	0.0001	1.668	20	3.16	8.87	0.03	0.086	0.99	0.935
3	Epsilon-SVR	Radial based	104	52562.3	1.88	-	0.026	5.37	7.28	0.052	0.07	0.972	0.949
4	Epsilon-SVR	Sigmoid	126	50000	0.028	0	0.0029	10.49	10.98	0.105	0.106	0.894	0.884
				C	Nu	Coeff0	Gamma						
5	Nu-SVR	Linear	116	216048	0.885	-	-	10.39	11.17	0.1	0.108	0.896	0.88
6	Nu-SVR	Polinomial degree = 3	32	38009.8	0.0069	2.281	0.159	6.132	8.107	0.059	0.078	0.964	0.937
7*	**Nu-SVR**	**Radial based**	**95**	**52229.2**	**-**	**-**	**0.025**	**5.36**	**7.21**	**0.052**	**0.069**	**0.972**	**0.95**
8	Nu-SVR	Sigmoid	117	59845.1	-	0	0.008	10.44	11.17	0.101	0.108	0.895	0.88

*Selected SVR model for parametric analysis

Among the produced models listed in Table 2, radial function based Nu-SVR model was selected for parametric study, as it performed the best as compared to other models. Fig. 7 shows the distribution obtained by the comparison of experimental and predicted data. Coefficient of determination (r-square, R^2) evaluates the linear relation between desired and output data (Eq. 9). Predicted and tested data appear to be aligned along the main diagonal of the graph, implying the ideal correspondence of predicted and tested data. Root mean squared error (*RMSE*) and coefficient of variation (CoV) were also calculated for testing and training sets of each model as listed in Table 2 (Eqs. 10-11). For proposed model (Model number 7, Nu-SVR-Radial based); R^2 value was calculated as **0.9784**. This indicates the high estimation capacity of proposed model. Other statistical measures were listen in Table A.1.

$$R^2 = 1 - \left(\frac{\sum_{i=1}^{N}(O_i - P_i)^2}{\sum_{i=1}^{N}(O_i - O_{ort.})^2} \right) \tag{9}$$

$$RMSE = \sqrt{\frac{\sum_{i=1}^{N}(P_i - O_i)^2}{N}} \tag{10}$$

$$Coefficient\ of\ Variation\ (CoV) = \frac{\sigma}{\overline{X}} \tag{11}$$

where N is the number of data, O_i is the experimental value of i_{th} data, P_i is the predicted value of i_{th} data, σ is the standard deviation and $\overline{X}$ is the mean value.
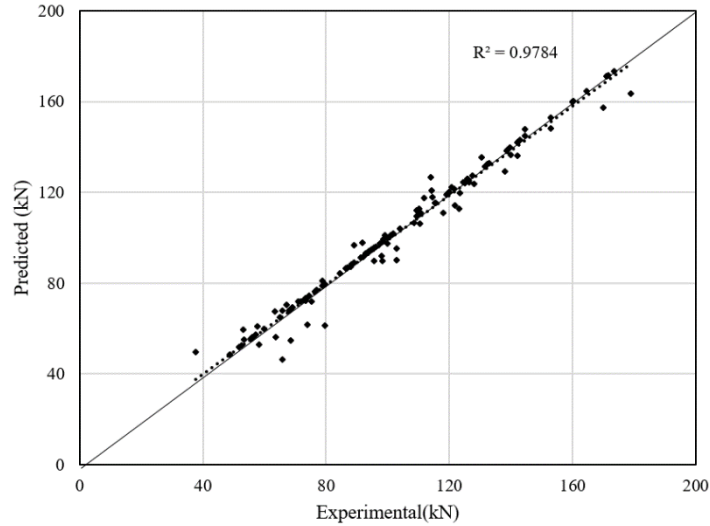
Figure 7. Comparison of SVR model results and experimental results.

Fig. 8. illustrates the performance of the model (Eq. 1) proposed by Fattuhi (1994). Although this model was created for the prediction of only SFRC corbel strength, we also used this model for GFRC corbels for comparison purposes. Large scattering of data is visible from Fig. 8a and Fig. 8b for SFRC and GFRC corbels, respectively. Coefficient of determination (R^2) of Fattuhi (1994) model (Eq. 1) was calculated as 0.8422 and 0.7245 for SFRC and GFRC corbels, respectively.
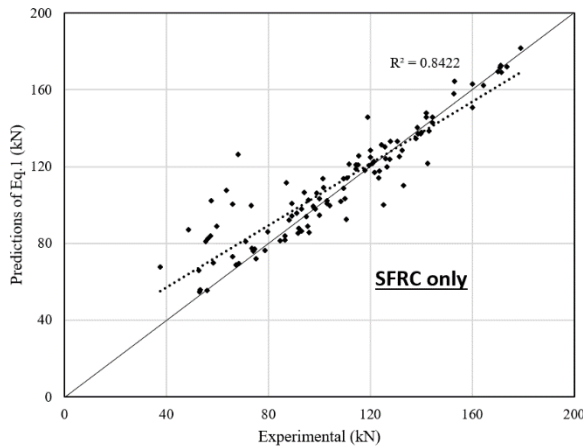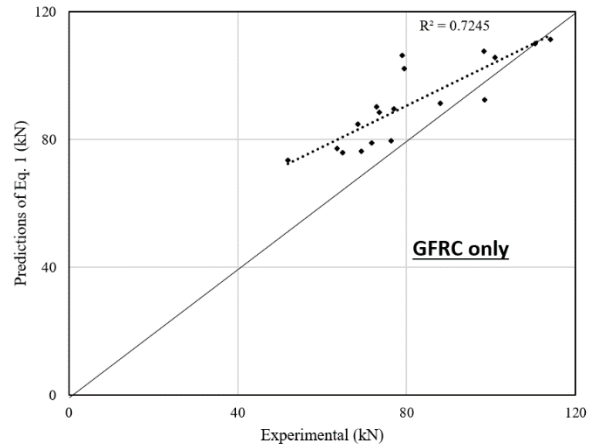
(a)	(b)

Figure 8. Performance of Fattuhi (1994) model [7] for (a) SFRC corbels (b) GFRC corbels.

Table A.1. Experimental database and comparison of model predictions

Source	Specimen	Fiber type	a/d	ρ (%)	f_y (MPa)	f_{cu} (Mpa)	f_t (MPa)	v_f (%)	V_{ke} (kN)	$V_{k,SVR}$ (kN)	$V_{k,Eq.1}$ (kN)	$V_{ke}/V_{k,SVR}$
Fattuhi and Hughes [3]	C2	Steel Fiber	1.04	0.70	558	53.51	4.37	0.7	84.50	84.50	81.23	1.00
	C3	Steel Fiber	1.05	0.71	558	52.60	5.45	0.7	92.90	92.90	86.21	1.00
	C4	Steel Fiber	1.02	0.70	558	51.40	4.79	0.7	91.80	97.96	85.29	0.94
	C5	Steel Fiber	1.05	0.71	558	51.10	5.36	0.7	96.00	95.88	85.64	1.00
	C6	Steel Fiber	1.07	0.69	558	40.10	3.19	0.7	75.20	71.87	71.81	1.05
Fattuhi and Hughes [4]	C27	Steel Fiber	0.43	0.45	495	47.30	4.64	0.7	125.80	125.80	130.15	1.00
	C28	Steel Fiber	0.72	0.45	495	55.70	6.09	0.7	88.20	88.20	92.31	1.00
	C29	Steel Fiber	0.96	0.44	495	55.70	6.09	0.7	65.90	46.53	73.06	1.42
	C30	Steel Fiber	0.43	0.70	558	51.40	4.79	0.7	171.00	171.00	171.50	1.00
	C31	Steel Fiber	0.55	1.02	491	57.00	5.05	0.7	179.00	163.48	181.89	1.09
	C32	Steel Fiber	1.06	1.00	491	47.30	4.64	0.7	110.10	112.86	103.25	0.98
Fattuhi and Hughes [5]	T3	Steel Fiber	0.73	0.70	558	47.90	4.66	0.7	133.00	133.00	110.10	1.00
	T4	Steel Fiber	0.72	0.71	558	55.90	6.19	1.4	142.50	142.50	121.80	1.00
	T6	Steel Fiber	0.72	0.70	537	57.40	9.28	2.1	143.00	143.00	138.49	1.00
	T10	Steel Fiber	0.76	1.02	491	47.90	4.66	0.7	138.00	129.12	134.52	1.07
	T11	Steel Fiber	0.74	1.02	491	55.90	6.19	1.4	160.20	160.20	150.76	1.00
	T12	Steel Fiber	0.74	1.02	491	57.40	9.28	2.1	171.20	171.20	172.83	1.00
Fattuhi [6]	1	Steel Fiber	0.65	1.00	452	41.40	5.84	1.7	153.00	153.00	164.50	1.00
	2	Steel Fiber	0.65	0.98	449	43.40	5.44	1.7	160.00	160.00	163.10	1.00
	3	Steel Fiber	0.63	0.44	451	42.00	4.86	1.7	91.20	91.20	95.64	1.00
	4	Steel Fiber	0.64	0.44	451	40.60	5.30	1.7	93.00	93.00	97.93	1.00
	5	Steel Fiber	1.14	0.98	452	40.51	5.46	1.7	103.00	95.40	102.34	1.08
	6	Steel Fiber	1.13	0.98	452	38.00	5.35	1.7	95.70	95.70	102.42	1.00
	7	Steel Fiber	1.11	0.44	451	33.80	3.89	0.7	53.30	55.25	55.93	0.96
	8	Steel Fiber	1.12	0.44	451	36.90	3.72	0.7	53.10	59.47	54.84	0.89
	9	Steel Fiber	0.65	1.00	452	34.51	5.29	1.7	152.90	148.26	158.03	1.03
	10	Steel Fiber	1.14	0.98	452	37.10	5.24	1.7	102.90	90.22	100.91	1.14
	11	Steel Fiber	1.11	0.44	451	35.80	3.76	0.7	56.00	56.00	55.49	1.00
	12	Steel Fiber	0.64	0.44	451	38.00	3.89	0.7	92.00	91.74	87.98	1.00
	13	Steel Fiber	0.89	0.99	452	34.00	5.04	1.7	111.70	117.36	121.40	0.95
	14	Steel Fiber	0.88	0.44	451	36.51	4.24	0.7	68.30	68.30	69.44	1.00
	15	Steel Fiber	0.87	0.44	451	39.00	3.92	0.7	67.20	70.40	68.57	0.95
	16	Steel Fiber	0.89	0.98	452	37.70	4.94	1.7	114.30	120.81	120.79	0.95
	18	Steel Fiber	0.71	0.99	452	32.60	4.98	1.0	119.00	119.00	145.72	1.00
Fattuhi [7]	20	Steel Fiber	0.89	0.99	452	38.60	5.43	1.8	126.00	126.00	124.16	1.00
	21	Steel Fiber	0.90	0.98	452	37.00	4.73	1.5	118.00	111.13	117.93	1.06
	22	Steel Fiber	0.81	0.69	454	37.00	4.73	1.5	108.50	106.60	101.76	1.02
	23	Steel Fiber	0.90	1.00	452	33.80	5.12	2.0	126.50	124.31	120.02	1.02
	24	Steel Fiber	0.65	0.69	454	33.80	5.12	2.0	131.50	131.50	125.19	1.00
	27	Steel Fiber	0.65	0.99	452	42.30	6.29	2.5	171.50	171.50	169.25	1.00
	28	Steel Fiber	0.48	0.68	454	42.30	6.29	2.5	173.50	173.50	171.94	1.00

	29	Steel Fiber	0.61	0.45	451	37.30	4.42	1.0	100.00	100.00	94.78	1.00
	30	Steel Fiber	1.00	0.70	454	37.30	4.42	1.0	86.50	86.50	83.74	1.00
	31	Steel Fiber	1.09	1.19	452	40.60	5.50	2.0	119.50	119.50	120.53	1.00
	32	Steel Fiber	1.00	1.23	452	40.60	5.50	2.0	132.50	132.50	128.31	1.00
	35	Steel Fiber	1.10	1.48	452	38.70	4.91	1.5	124.50	124.50	131.19	1.00
	36	Steel Fiber	0.49	0.44	451	38.70	4.91	1.5	123.50	119.68	117.75	1.03
	37	Steel Fiber	1.10	1.49	452	39.60	5.72	2.0	140.00	136.48	137.86	1.03
	38	Steel Fiber	0.89	0.44	451	39.60	5.72	2.0	74.00	61.58	75.96	1.20
	39	Steel Fiber	0.89	1.20	452	38.70	5.64	2.3	144.50	144.94	142.75	1.00
	40	Steel Fiber	1.02	1.47	452	38.70	5.64	2.3	142.00	136.07	145.83	1.04
	44	Steel Fiber	1.10	1.21	452	35.40	4.85	1.5	109.50	111.94	113.82	0.98
	45	Steel Fiber	1.10	1.50	452	34.80	4.37	1.0	120.00	120.00	124.96	1.00
	46	Steel Fiber	0.82	0.45	451	34.80	4.37	1.0	74.50	74.50	77.04	1.00
	48	Steel Fiber	0.86	0.68	454	35.70	5.16	2.0	100.00	97.32	103.39	1.03
	49	Steel Fiber	0.66	1.00	452	37.60	5.81	2.5	164.50	164.50	162.47	1.00
	51	Steel Fiber	0.83	1.00	451	38.60	5.83	2.0	130.50	135.23	133.10	0.97
	52	Steel Fiber	1.17	1.00	451	38.60	5.83	2.0	99.00	101.24	106.00	0.98
	53	Steel Fiber	1.01	1.48	451	41.10	5.68	2.0	144.50	147.77	145.78	0.98
	54	Steel Fiber	1.44	1.49	451	41.10	5.68	2.0	101.50	101.50	113.85	1.00
	55	Steel Fiber	0.55	0.44	451	36.90	4.06	1.0	104.00	104.00	99.57	1.00
	56	Steel Fiber	0.65	0.44	451	36.90	4.06	1.0	95.50	89.68	88.78	1.06
	57	Steel Fiber	0.59	0.69	451	38.80	5.92	2.0	138.50	138.50	140.30	1.00
	58	Steel Fiber	0.71	0.69	451	38.80	5.92	2.0	121.50	121.39	122.55	1.00
	59	Steel Fiber	1.18	0.99	451	36.20	5.37	2.0	97.50	97.50	99.50	1.00
	60	Steel Fiber	0.98	1.49	451	36.20	5.37	2.0	142.00	142.00	148.04	1.00
	61	Steel Fiber	0.63	0.44	451	36.30	4.82	1.5	98.50	99.17	97.76	0.99
	62	Steel Fiber	1.18	1.20	451	36.30	4.82	1.5	109.50	109.50	108.57	1.00
	63	Steel Fiber	0.85	0.68	451	38.20	5.94	2.5	101.80	101.80	109.06	1.00
Fattuhi [8]	64	Steel Fiber	0.65	1.00	451	38.20	5.94	2.5	170.00	157.15	169.37	1.08
	75	Steel Fiber	0.60	0.44	451	31.00	4.05	1.0	94.80	94.78	93.79	1.00
	76	Steel Fiber	0.79	0.44	451	31.00	4.05	1.0	73.50	73.50	77.28	1.00
	77	Steel Fiber	0.90	1.00	451	33.20	4.96	1.5	114.50	117.79	118.63	0.97
	78	Steel Fiber	1.11	1.50	451	33.20	4.96	1.5	120.00	120.00	128.45	1.00
	79	Steel Fiber	1.09	1.48	451	33.80	5.26	2.0	128.00	123.80	133.29	1.03
	80	Steel Fiber	0.90	1.00	451	33.80	5.26	2.0	120.80	122.10	121.47	0.99
	81	Steel Fiber	1.11	1.22	451	35.40	5.04	2.0	110.80	110.80	114.08	1.00
	82	Steel Fiber	1.20	1.00	451	35.40	5.04	2.0	98.00	91.82	98.76	1.07
	83	Steel Fiber	1.21	1.53	451	34.90	4.96	1.5	115.30	115.30	120.98	1.00
	84	Steel Fiber	1.47	1.51	451	34.90	4.96	1.5	94.00	94.00	106.39	1.00
	85	Steel Fiber	0.98	0.99	451	35.10	5.17	2.0	123.30	112.95	114.02	1.09
	86	Steel Fiber	1.19	1.48	451	35.10	5.17	2.0	115.50	115.50	125.61	1.00
	87	Steel Fiber	0.64	0.69	451	36.20	6.01	2.5	139.80	139.80	137.14	1.00
	88	Steel Fiber	0.86	1.00	451	36.20	6.01	2.5	138.80	138.80	137.04	1.00
	50-0-10-100	Steel Fiber	0.82	0.86	560	48.15	3.10	0.0	65.91	67.84	100.28	0.97
	50-0-10-130	Steel Fiber	1.06	0.85	560	48.15	3.10	0.0	55.52	55.52	80.94	1.00

	50-0-12-100	Steel Fiber	0.81	1.22	510	47.53	3.10	0.0	68.06	68.06	126.29	1.00
	50-0-12-130	Steel Fiber	1.02	1.18	510	47.53	3.10	0.0	57.65	61.04	102.23	0.94
	50-1-10-100	Steel Fiber	0.83	0.70	560	50.00	3.70	1.0	110.58	106.25	92.59	1.04
Kurtoglu	50-1-10-130	Steel Fiber	1.05	0.70	560	50.00	3.70	1.0	78.80	78.80	76.22	1.00
[14]	50-1-12-100	Steel Fiber	0.82	1.01	510	50.00	3.60	1.0	121.78	114.16	116.81	1.07
	50-1-12-130	Steel Fiber	1.07	1.01	510	50.00	3.60	1.0	89.18	89.13	94.16	1.00
	50-1.5-10-100	Steel Fiber	0.81	0.70	560	50.00	4.50	1.5	125.13	124.05	100.12	1.01
	50-1.5-10-130	Steel Fiber	1.04	0.70	560	50.00	4.50	1.5	86.58	86.58	81.59	1.00
	50-1.5-12-100	Steel Fiber	0.81	1.01	510	50.00	4.20	1.5	127.54	127.54	123.65	1.00
	50-1.5-12-130	Steel Fiber	1.04	1.01	510	50.00	4.20	1.5	89.13	96.66	100.77	0.92
	30-0-10-100	Steel Fiber	0.81	0.85	560	30.00	1.90	0.0	57.22	57.22	83.88	1.00
	30-0-10-130	Steel Fiber	1.06	0.85	560	30.00	1.90	0.0	37.57	49.82	67.78	0.75
	30-0-12-100	Steel Fiber	0.81	1.22	510	30.00	2.00	0.0	63.53	56.12	107.55	1.13
	30-0-12-130	Steel Fiber	1.04	1.21	510	30.00	2.00	0.0	48.65	48.65	87.20	1.00
	30-1-10-100	Steel Fiber	0.81	0.70	560	30.00	2.50	1.0	71.00	72.00	81.14	0.99
	30-1-10-130	Steel Fiber	1.05	0.70	560	30.00	2.50	1.0	52.60	52.60	65.70	1.00
	30-1-12-100	Steel Fiber	0.81	1.01	510	30.00	2.30	1.0	73.39	72.30	99.75	1.02
	30-1-12-130	Steel Fiber	1.02	1.01	510	30.00	2.30	1.0	56.15	56.15	82.37	1.00
	30-1.5-10-100	Steel Fiber	0.82	0.70	560	30.00	3.10	1.5	79.66	79.66	86.11	1.00
	30-1.5-10-130	Steel Fiber	1.06	0.70	560	30.00	3.10	1.5	58.35	53.02	69.85	1.10
	30-1.5-12-100	Steel Fiber	0.79	1.01	510	30.00	3.10	1.5	87.01	87.01	111.46	1.00
	30-1.5-12-130	Steel Fiber	1.05	1.01	510	30.00	3.10	1.5	59.79	59.79	88.73	1.00
	S8-80	Glass Fiber	0.66	0.53	550	102.66	4.79	0.0	100.95	100.95	105.73	1.00
	S8-100	Glass Fiber	0.84	0.56	550	102.66	4.79	0.0	72.80	72.80	90.29	1.00
	S8-120	Glass Fiber	0.99	0.53	550	102.66	4.79	0.0	64.90	64.90	75.98	1.00
	S8-80-0.2	Glass Fiber	0.63	0.53	550	96.15	4.99	0.2	110.50	110.50	110.05	1.00
	S8-100-0.2	Glass Fiber	0.80	0.54	550	96.15	4.99	0.2	88.00	87.35	91.37	1.01
	S8-120-0.2	Glass Fiber	0.95	0.53	550	96.15	4.99	0.2	71.80	71.80	78.90	1.00
	S8-80-0.4	Glass Fiber	0.63	0.53	550	98.69	5.14	0.4	114.00	126.49	111.23	0.90
	S8-100-0.4	Glass Fiber	0.80	0.54	550	98.69	5.14	0.4	98.50	98.50	92.35	1.00
	S8-120-0.4	Glass Fiber	0.96	0.54	550	98.69	5.14	0.4	76.30	76.30	79.64	1.00
	S8-A80	Glass Fiber	0.66	0.55	550	70.50	4.21	0.0	79.50	61.25	102.11	1.30
	S8-A100	Glass Fiber	0.83	0.55	550	70.50	4.21	0.0	68.50	54.74	84.84	1.25
	S8-A120	Glass Fiber	0.99	0.55	550	70.50	4.21	0.0	51.85	51.85	73.47	1.00
	S8-A80 – 0.2%	Glass Fiber	0.63	0.53	550	63.71	4.78	0.2	78.90	80.93	106.41	0.97
	S8-A100 -0.2%	Glass Fiber	0.79	0.53	550	63.71	4.78	0.2	73.50	73.50	88.58	1.00
	S8-A120-0.2%	Glass Fiber	0.95	0.53	550	63.71	4.78	0.2	69.20	69.20	76.28	1.00
	S8-A80-0.4%	Glass Fiber	0.63	0.53	550	68.84	4.91	0.4	98.30	89.67	107.72	1.10
	S8-A100-0.4%	Glass Fiber	0.79	0.53	550	68.84	4.91	0.4	77.00	77.00	89.67	1.00
	S8-A120 -0.4%	Glass Fiber	0.95	0.53	550	68.84	4.91	0.4	63.50	67.42	77.22	0.94

Mean	1.01
St. Dev.	0.07
CoV	0.07
R^2	0.9784

5. PARAMETRIC ANALYSIS

A parametric analysis was conducted in order to survey the generalization capability of proposed models. A database was created by determining 2 values for fiber type (categorical variable) and 3 values for each input variable (6 variables). Thus, $2^1 \times 3^6 = 1458$ rows of data were created using a Matlab code, prepared for parametric data generation. These values were kept in the range of each parameter as listed in Table 1. The database was then used for scoring each model and effect of each parameter was observed on the output.

Main effect graph (Fig. 9) is a significant tool to observe whether the model works for the input data different than test data.

Fig. 9 depicts that the trend of each parameter confirms the literature and they are found as expected, which approves the generalization capability of proposed model.

As shown in main effect graphs (Fig. 9), span-to-depth ratio *a/d* has most dominant effect on the shear strength of FRC corbels. Shear-span-to-depth ratio has inversely proportional effect, which confirms the literature [25]. Additionally, reinforcement ratio (ρ), compressive and tensile strengths of concrete (f_{cu} and f_t) and volume fiber ratio (v_f) shows directly proportional effect on the shear strength. On the other hand, tensile strength of steel reinforcement (f_y) demonstrates almost no effect, which can be attributable to the fact that the steel reinforcements reached the maximum yield strength before the corbel's ultimate load capacity.
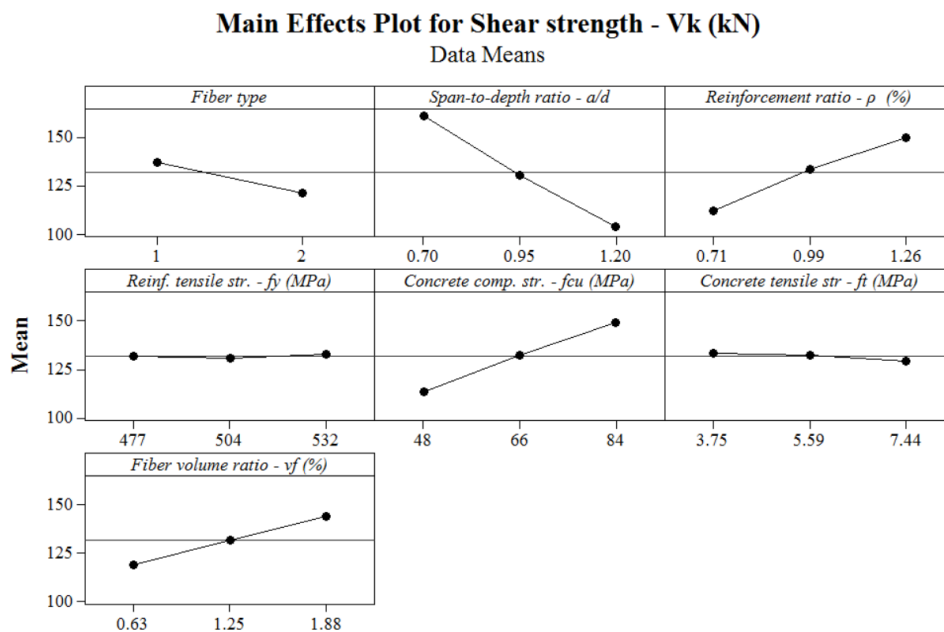

Figure 9. Effects of input variables on shear strength of FRC corbels.

Fig. 10 shows the interactive effect of two input parameters on output parameter (shear strength). Effect of increasing reinforcement ratio yields greater shear strength and this effect is greater for lower shear span-to-depth ratio values (Fig. 10a). Similar effect is visible for combined effect

of compressive strength and span-to-depth ratio on shear strength (Fig. 10b). On the other hand, higher span-to-depth ratio values result in lower shear strength (Fig. 10c). Increase in reinforcement tensile strength does not have a significant effect on shear strength, which is

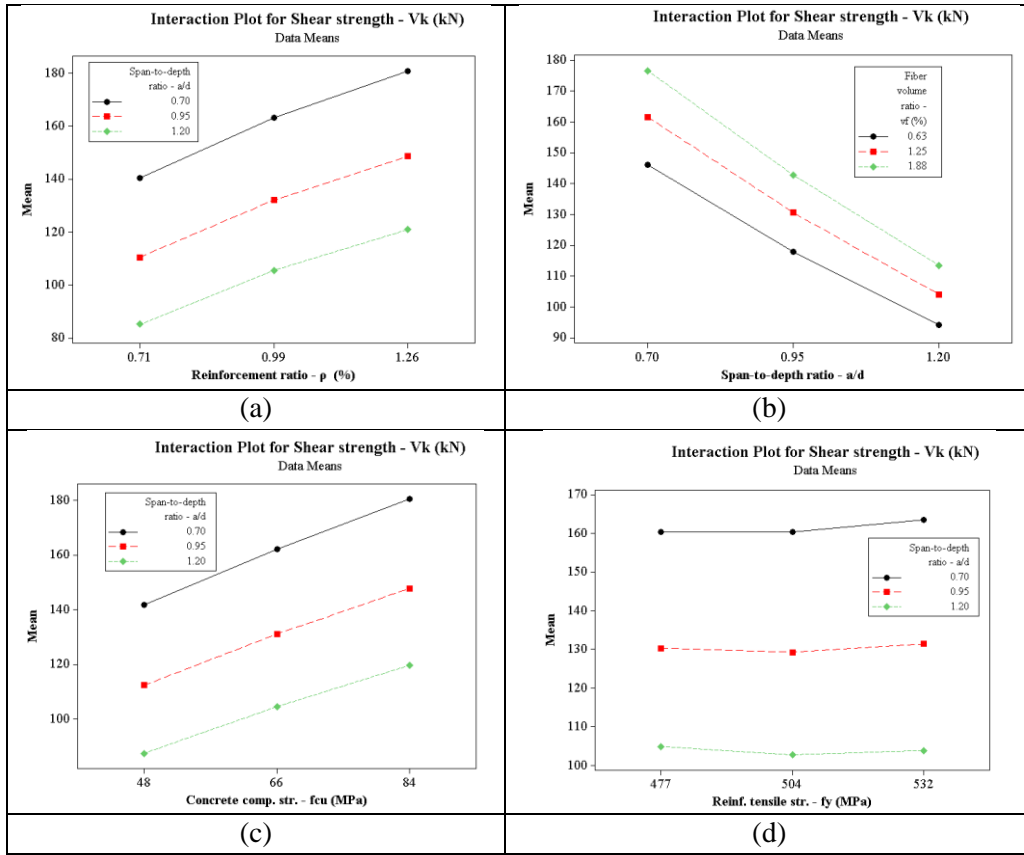pronounced more for greater shear span-to-depth
ratios (Fig. 10d).

Figure 10. Interactive effect of inputs on shear strength of FRC corbels.

6. CONCLUSION

Precast corbels are the structural members commonly preferred in industrial buildings. This paper proposes a support vector machines (SVM) based model to predict the ultimate load capacity of fiber reinforced concrete (FRC) corbels, for the first time in literature. SVM was also employed in many structural engineering problems [24]. A wide range of database with existing test results was established and multiple SVM models were created. Among the models, best performing one was selected and the results were compared to an existing model. Furthermore, selected model was tested by means of a parametric study to figure out the prediction capacity for input values different than experimental data. In models, input parameters were fiber type (steel fiber and glass fiber), span-to-depth ratio (a/d), steel reinforcement ratio (ρ), steel reinforcement tensile strength (f_y), concrete compressive strength (f_{cu}), concrete tensile strength (f_t) and fiber volume ratio (v_f). Based on these findings mentioned above, following conclusion can be drawn:

- Proposed model shows high prediction performance on estimating the test results for shear strength of both SFRC and GFRC simply supported corbels with various geometry and material properties.
- Parametric analysis' results suggest that the model has the generalization capability, which implies that the model functions successfully for not only the provided test data but also the data generated within the range of input variables.
- It can be stated that the span-to-depth ratio (a/d) has dominant effect on ultimate load capacity.
- Encouraging performance of support vector machines approach in solving complex problems can draw attentions of engineers and researchers, being a robust and successful alternative.

REFERENCES

[1]. American Concrete Institute, State-of-the-Art Report on Fiber Reinforced Concrete. ACI Committee 544, 2002.

[2]. Fanella D.A. and Naaman A.E., Stress-Strain Properties of Fiber Reinforced Mortar in Compression, J. Amer. Concr. Inst., 82 (1985) 475-483.

[3]. Thomas J. and Ramaswamy A., Mechanical Properties of Steel Fiber-Reinforced Concrete, J. Mater. Civ. Eng., 19 (2007) 385-392.

[4]. Deluce J.R., Cracking Behaviour of Steel Fibre Reinforced Concrete Containing Conventional Steel Reinforcement. MSc Thesis, 2011.

[5]. Fattuhi N.I., SFRC Corbel Tests, ACI Struct. J., 84 (1987) 119-123.

[6]. Fattuhi N.I., Column-Load Effect on Reinforced Concrete Corbels, J. Struct. Eng., 116 (1990) 188-197.

[7]. Fattuhi N.I., Strength of FRC Corbels in Flexure, J. Struct. Eng., 120 (1994) 360-377.

[8]. Fattuhi N.I. and Hughes B.P., Ductility of Reinforced Concrete Corbels Containing Either Steel Fibers or Stirrups, ACI Struct. J., 86 (1989) 644-651.

[9]. Fattuhi N.I and Hughes B.P., Reinforced Steel Fiber Concrete Corbels with Various Shear Span-To-Depth Ratios, ACI Mater. J., 86 (1989) 590-596.

[10]. Campione G., La Mendola L., Mangiavillano M.L., Steel fiber-Reinforced Concrete Corbels: Experimental Behavior and Shear Strength Prediction, ACI Struct. J., 104 (2007) 570-579.

[11]. Campione G., Performance of Steel Fibrous Reinforced Concrete Corbels Subjected to Vertical and Horizontal Loads, J. Struct. Eng., 135 (2009) 519-529.

[12]. Muhammad A., Behavior and Strength of High-Strength Fiber Reinforced Concrete Corbels Subjected to Monotonic or Cyclic (Repeated) Loading, PhD thesis, Dept. of

Building and Construction Eng., University of Technology, Baghdad, 1998.

[13]. Yang J.M., Lee J.H., Yoon, Y.S., Cook W.D., Mitchell D., Influence of Steel Fibers and Headed Bars on The Serviceability of High-Strength Concrete Corbels, J. Struct. Eng., 138 (2011) 123-129.

[14]. Kurtoglu A.E., Gulsan M.E., Abdi H.A., Kamil M.A., Cevik A., Fiber Reinforced Concrete Corbels: Modeling Shear Strength Via Symbolic Regression. Comp. and Concr., 20 (2017) 1-10.

[15]. Boser B.E., Guyon I.M., Vapnik V.N., A Training Algorithm for Optimal Margin Classifiers, Proceedings of The Fifth Annual Workshop on Computational Learning Theory, (1992) 144-152.

[16]. Wang, L., (Ed). Support Vector Machines: Theory and Applications. Berlin: Springer, 2005.

[17]. Chen N., Lu W., Yang J., Li G., (Eds). Support Vector Machine in Chemistry. World Scientific, 2004.

[18]. Cherkassky V. and Ma Y., Selection of Meta-Parameters for Support Vector Regression, Artificial Neural Networks - ICANN 2002, (2002) 687-693.

[19]. Zhang W. and Song Z., Prediction of Concrete Corrosion in Sulfuric Acid by SVM-Based Method, 2nd International Conference on Electronic and Mechanical Engineering and Information Technology, 2012.

[20]. Yang S., Fang C.Q., Yuan Z.J., Study on Mechanical Properties of Corroded Reinforced Concrete Using Support Vector Machines, Appl. Mech. and Mater., 578 (2014) 1556-1561.

[21]. Cao Y.F., Wu W., Zhang H.L., Pan J.M., Prediction of the Elastic Modulus of Self-Compacting Concrete Based on SVM, Appl. Mech. and Mater., 357 (2013) 1023-1026.

[22]. Li H.S., Lu Z.Z., Yue, Z.F., Support Vector Regression for Structural Reliability Analysis, Appl. Math. and Mech., 27 (2006) 1295-1303.

[23]. Okkan U., Serbes Z.A., Rainfall–Runoff Modeling Using Least Squares Support Vector Machines, Environmetrics, 23 (2012) 549-564.

[24]. Çevik A., Kurtoğlu A.E., Bilgehan M., Gülşan M.E., Albegmprli H.M., Support Vector Machines in Structural Engineering: A Review, J. Civil Eng. and Manag., 21 (2015) 261-281.

[25]. Kumar S., Barai S., Neural Networks Modeling of Shear Strength of SFRC Corbels Without Stirrups, Appl. Soft Comput., 10 (2010) 135-148.

[26]. Sherrod P.H., DTREG Predictive Modeling Software, Users Manual, 2008.